Description of morphological evolution of lung tumors treated by percutaneous radiofrequency ablation: long term follow-up of 100 lesions with chest CT

Paul Habert, Mathieu Di Bisceglie, Axel Bartoli, Alexis Jacquier, Pauline Brige, Vincent Vidal, Jean-François Hak, Farouk Tradi, Jean-Yves Gaubert

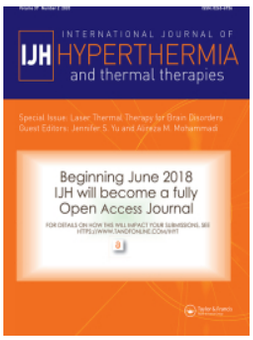

Taylor & Francis
Taylor & Francis Group

International Journal of Hyperthermia

ISSN: (Print) (Online) Journal homepage: https://www.tandfonline.com/loi/ihyt20

Description of morphological evolution of lung tumors treated by percutaneous radiofrequency ablation: long term follow-up of 100 lesions with chest CT

Paul Habert, Mathieu Di Bisceglie, Axel Bartoli, Alexis Jacquier, Pauline Brige, Vincent Vidal, Jean-François Hak, Farouk Tradi & Jean-Yves Gaubert

To cite this article: Paul Habert, Mathieu Di Bisceglie, Axel Bartoli, Alexis Jacquier, Pauline Brige, Vincent Vidal, Jean-François Hak, Farouk Tradi & Jean-Yves Gaubert (2021) Description of morphological evolution of lung tumors treated by percutaneous radiofrequency ablation: long term follow-up of 100 lesions with chest CT, International Journal of Hyperthermia, 38:1, 786-794, DOI: 10.1080/02656736.2021.1928773

To link to this article: https://doi.org/10.1080/02656736.2021.1928773

Published online: 25 May 2021.

INTERNATIONAL JOURNAL OF HYPERTHERMIA
2021, VOL. 38, NO. 1, 786–794
https://doi.org/10.1080/02656736.2021.1928773

Description of morphological evolution of lung tumors treated by percutaneous radiofrequency ablation: long term follow-up of 100 lesions with chest CT

Paul Habert[a,b,c], Mathieu Di Bisceglie[a,b,c], Axel Bartoli[a,d], Alexis Jacquier[a,d], Pauline Brige[b,c], Vincent Vidal[a,b,c], Jean-François Hak[a,b,c], Farouk Tradi[a,b,c] and Jean-Yves Gaubert[a,b,c]

[a]Department of Medical Imaging, La Timone Hôpital, Marseille, France; [b]LIIE, Aix Marseille University, Marseille, France; [c]CERIMED, Aix Marseille University, Marseille, France; [d]Centre d'exploration métabolique par résonnance magnétique CEMEREM, Aix-Marseille Université, Marseille, France

ABSTRACT

Purpose: Radiofrequency ablation (RFA) is a safe and effective minimally invasive treatment for pulmonary tumors. Patterns on chest computed tomography (CT) after RFA are classified into five types; however, the follow-up has not been fully described. The objectives of this study were to describe (1) the CT pattern 3 years after RFA and (2) its evolution over 7 years.

Materials and methods: Lesions treated with RFA between 2009 and 2017 and with ≥3 years of follow-up CT data were included. Lesions with local recurrences were excluded from the study. The morphology of the ablation zone was classified as nodular, fibrotic, atelectatic, cavitary, and disappeared. Other initial anatomical parameters were recorded. Kruskal–Wallis or Chi-square tests were used to compare the groups.

Results: One hundred lung RFA scars were included, and a retrospective longitudinal study was performed. Three years after RFA, nodular, fibrotic, atelectatic, and cavitary scars, and disappearance were observed in 49%, 36%, 5%, 3%, and 6% of the scars, respectively. Evolution over 7 years showed that the fibrosis, atelectasis, and disappearance remained stable over time, whereas 28% of nodular scars evolved into fibrotic scars. Additionally, 45% of cavitary scars evolved into nodular scars. Pleural contact was associated with disappearance, and the use of a 20-mm needle was associated with atelectasis.

Conclusion: Follow-up after RFA showed that fibrosis, disappearance, and atelectasis remained stable over time. Nodular scars could evolve into fibrotic scars, and cavitary scars could evolve into nodular scars.

ARTICLE HISTORY
Received 4 November 2020
Revised 2 May 2021
Accepted 6 May 2021

KEYWORDS
Interventional radiology; lung metastases; primary lung tumor; radiofrequency ablation; computed tomography; follow-up

Introduction

Radiofrequency ablation (RFA) of primary and secondary lung tumors has two advantages: it is a minimally invasive curative procedure and has a very low rate of complications [1]. A radiofrequency wave causes ionic stirring and an increase in temperature in the tumor, resulting in immediate cell death by coagulation and necrosis, and delayed cell death by apoptosis [2]. The doses received by operators are within the recommended standards and do not represent a limit to the practice of RFA [3], according to recently published guidelines [4]. The first pulmonary RFA procedure was described in 2000 [5], and multiple studies have shown low rates of complications [6–8]. Local tumor control is comparable to wedge resection or stereotactic body radiation therapy for metastasis [9,10]. Recent guidelines for colorectal cancer metastases clearly indicate that ablation is recommended as a free-standing therapy or in combination with resection, whereas stereotactic body radiation therapy is indicated only for selected patients not amenable to resection or within a clinical trial [11]. In primary lung cancer stage 1 A, a phase II study found overall survivals of 84% and 81% at 1 and 3 years, respectively [12]. Moreover, RFA is feasible even in single-lung patients [13].

Despite these advantages, RFA is still underutilized, and the poorly standardized morphological follow-up could be one of the pitfalls of this technique. Early detection of local recurrence is key because it can be retreated using RFA. Normal morphological local evolution 1 year after treatment has been described and classified in 2011 into five types based on radiographic appearance: fibrosis, nodular scars, atelectasis, cavitary scars, and disappearance [14]. This study aimed to describe the long-term morphological evolution of scars on computed tomography (CT) after RFA, with at least 3 years of follow-up, and to evaluate the impact of different initial anatomical parameters on the morphology at the 3-year follow-up.

CONTACT Paul Habert paul.habert@ap-hm.fr Department of Medical Imaging, La Timone Hôpital, 267, rue Saint-Pierre, Marseille 13005, France

Materials and methods

Population

We retrospectively collected data from patients who underwent RFA between December 2009 and June 2017 and met the following inclusion criteria: underwent RFA of one or more lung tumors, with available medical follow-up data, including regular chest CT scans for at least 3 years after RFA at our institution. The exclusion criteria were as follows: unavailable chest CT data, surgery after RFA, resulting in scar removal or disease progression that did not allow an appropriate analysis of the scar. The protocol was approved by the institutional review board 'Comité d'Ethique pour la recherche en Imagerie Médicale' n°CRM-2010-112.

RFA

All indications for RFA were decided by a multidisciplinary team involving radiologists, thoracic surgeons, oncologists, pneumologists, radiation therapists, and pathologists. Patients were eligible for treatment if they had fewer than five lesions, the lesions were not in contact with a vessel with a diameter >4 mm, and the lesions were not in contact with the proximal main bronchus. All procedures were performed under general anesthesia and CT guidance by an experienced interventional radiologist with 10 years of experience in RFA (JYG), with monitoring of the patients' vital signs. Two grams of amoxicillin-clavulanate was administered during the intervention and for 5 days postoperatively. RFA was performed using a 15-gauge radiofrequency needle with a coaxial system (LeVeen CoAccess needle, Boston Scientific, Natick, MA, USA). The size of the active radiofrequency portion of the needle was chosen according to the size of the lesion to be treated (10 mm > the size of the lesion to control lateral margins, considering a safe margin of 5 mm; range of the desired ablation zone, 20–40 mm) [15,16]. An RFA generator (RF2000, Boston Scientific) was used to progressively increase the power according to the following model: 5 W initially, increased by 5 W every 2 min until 30 W. Thereafter, it was increased by 5 W every minute until 50 W, and finally by 10 W every minute until a roll-off was obtained. A second ablation was performed after a 2-min pause, starting at half the power of the previous roll-off. The same method for power increase was used until a new roll-off occurred.

CT evaluation and follow-up

All patients underwent chest CT within a month before RFA and were followed up using chest CT. Each patient underwent chest CT a month after RFA, every 3 months during the first year, and every 6 months thereafter. Follow-up CT scans were systematically performed in a single center using a SOMATOM Definition AS + scanner (Siemens Healthineers, Erlangen, Germany) using the following parameters: 120 kV and 1 mAs/kg with CARE dose modulation and reconstruction in joint slices of 1:1 mm. We manually modified the dose according to the patient's weight: 140 kV or 100 kV if they weighed >120 kg or <60 kg, respectively. All thoracic scans from the adrenal glands to the neck were acquired during breath-hold inspiration, and chest CT scans were acquired with contrast injection if there was no contraindication. The enhancement was used to detect nodular enhancement or mediastinal lymph nodes.

Image analysis

CT scans of all patients were retrieved from archiving software and medical records and retrospectively analyzed. All chest CT scans were assessed independently by two trained chest radiologists, JYG and PH, with >25 and >10 years of experience, respectively. In case of disagreement, they reached a consensus. The following details were obtained from the initial chest CT scan: lesion size, contact with the pleura, and distance to the pleura if the lesion was fully surrounded by parenchyma. In addition, we obtained the power delivered locally in watts, and the origin of the primary tumor, if the lesion was a metastatic tumor, from the medical records. Forty-eight hours after RFA, the area of the ground glass opacity (GGO) surrounding the lesion was measured, and GGO at least 5 mm larger than the lesion was deemed to indicate a sufficient margin. The maximum diameter of the lesion in the axial plane on chest CT performed on the day of RFA was assessed, even if the lesion was irregular and included spikes in the case of primary lung cancer.

In the case of follow-up chest CT, the morphological evolution of the treated zone was classified into five types [14] (Figure 1) and evaluated every year according to the availability of chest CT data.

- Fibrosis: a band/atelectasis, with a tendency to stretch away from the ablation site.
- Nodule: of the same size, smaller, or often larger than the treated tumor during the first 6 months after RFA.
- Atelectasis: sagging of the parenchyma around the zone of ablation leading to subsegmental atelectasis.
- Cavitary: a cavity with a thin or thick wall.
- Disappearance.

Due to the retrospective design of the study and the loss of patients to follow-up, we obtained the year-by-year evolution of each lesion treated according to the chest CT data in the Picture Archiving and Communication System.

Statistical analysis

Normally distributed continuous data are expressed as the mean ± standard deviation, and non-normally distributed data are expressed as the median (range). Categorical data are expressed as frequencies or percentages. All data were analyzed using Prism 8 software (GraphPad Software, Inc.). The Kruskal–Wallis or Chi-square tests were used to compare differences between groups regarding the different preoperative parameters. Statistical significance was set at $p < 0.05$.

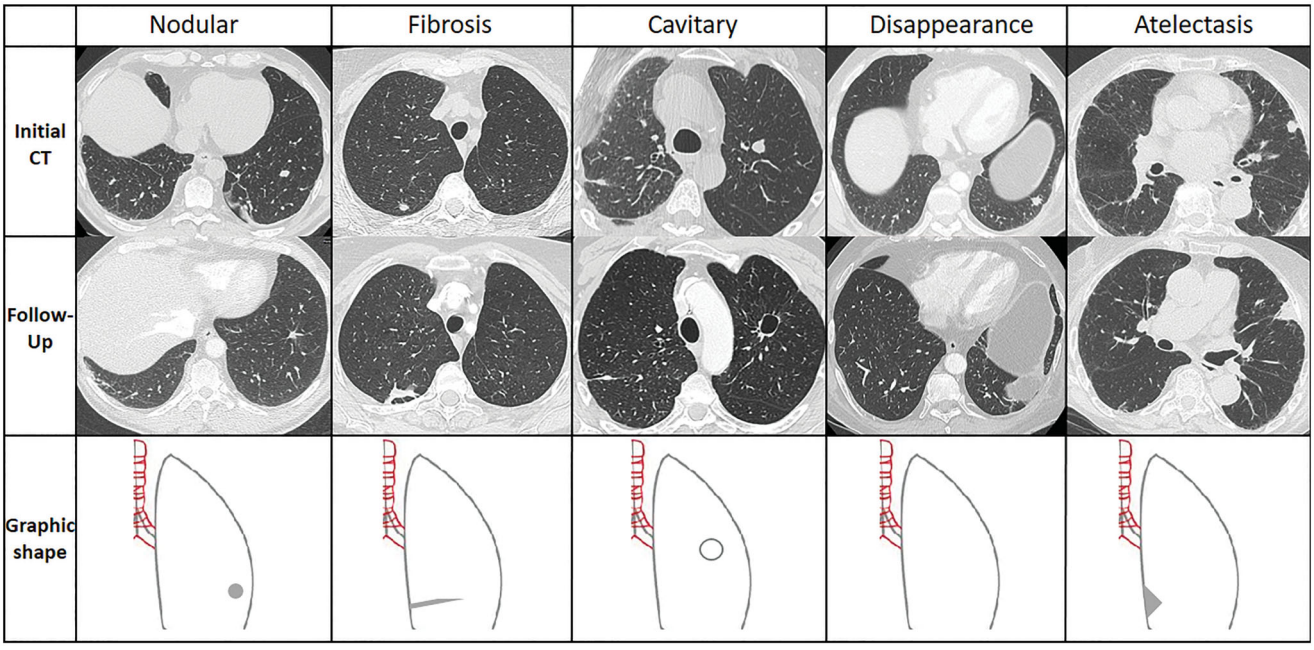

Figure 1. Representation of each type of scar 3 years after RFA. The top row shows the nodules before the treatment, the mid row shows the different kind of scars during follow-up after RFA and the bottom row a schematic drawing of the scar. Each column corresponds to one patient before and after RFA.

Results

Patients

One hundred lesions treated during the previously described period met the inclusion criteria. There were 41 lesions in men and 59 lesions in women, corresponding to 69 patients with a mean age of 62 ± 14 years (range, 23–88 years). Among the 100 initially included lesions, chest CT data at 1, 2, 3, 4, 5, 6, and 7 years after RFA were available for 93, 96, 93, 71, 49, 33, and 20 lesions, respectively (Figure 2).

Characteristics of the lesions

The mean lesion size was 14 ± 7 mm, with a median size of 12 mm. Most lesions were smaller than 20 mm (83%). The active radiofrequency diameter of the needle used for treatment was mostly 30 mm (49%) and ranged from 20 to 40 mm. All patients received two heat cycles; the mean power for the first roll-off was 61 ± 40 W, and the mean power for the second roll-off was 56 ± 41 W. The average power for the first and second heat cycles was 59 ± 38 W. Lesion with pleural contact was noted in 18% of the cases, and for the remaining 82%, the mean distance to the pleura was 12 ± 12 mm. The area of GGO measured on CT 48 h after RFA was 884 ± 392 mm. Primary lung cancer was treated in 16% of the cases, and 84% were metastatic diseases. The most frequent metastases were metastatic sarcomas (37%) and colorectal cancers (29%) (Table 1).

Distribution of scars 3 years after RFA

Chest CT data at the 3-year follow-up were available for 96 treated lesions. At 3 years, the distribution of different scars was as follows: nodular, 49%; fibrotic, 36%; atelectatic, 6%; cavitary, 5%; disappeared, 3%.

Evolution of scars over time

The maximum follow-up duration for CT was 7 years in 20 lesions. The morphology was most frequently nodular or fibrotic; however, the frequency of the patterns changed over time; in the first 3 years, nodular scars were dominant, and thereafter, fibrosis was dominant (Table 2). The proportion of cavitary scars, atelectasis, and disappearance was approximately stable in the first 5 years.

Curves following the evolution of different patterns over time showed that fibrosis, atelectasis, and disappearance did not change with time (Figure 3). Nodular scars tended to transform into fibrotic scars with time, with 50% of nodular scars becoming fibrotic within 5 years after RFA (Figure 4) and <10% becoming cavitary. Thirty percent of the cavitary scars in this study evolved into nodular scars (Figure 3).

Evolution of scars according to lesion or RFA parameters

There was no significant difference between the scar groups regarding lesion size, power delivery, GGO area measured on chest CT 48 h after RFA, sufficient margins, or lesion type. Thus, none of these factors predicted scar evolution. The lesions located close to the pleura more frequently disappeared than evolving into nodular scars ($p = 0.04$) (Figures 5 and 6).

Lesions evolved into atelectasis only if they measured <20 mm ($p < 0.001$). Consequently, atelectasis was more frequently associated with the use of a 20-mm active

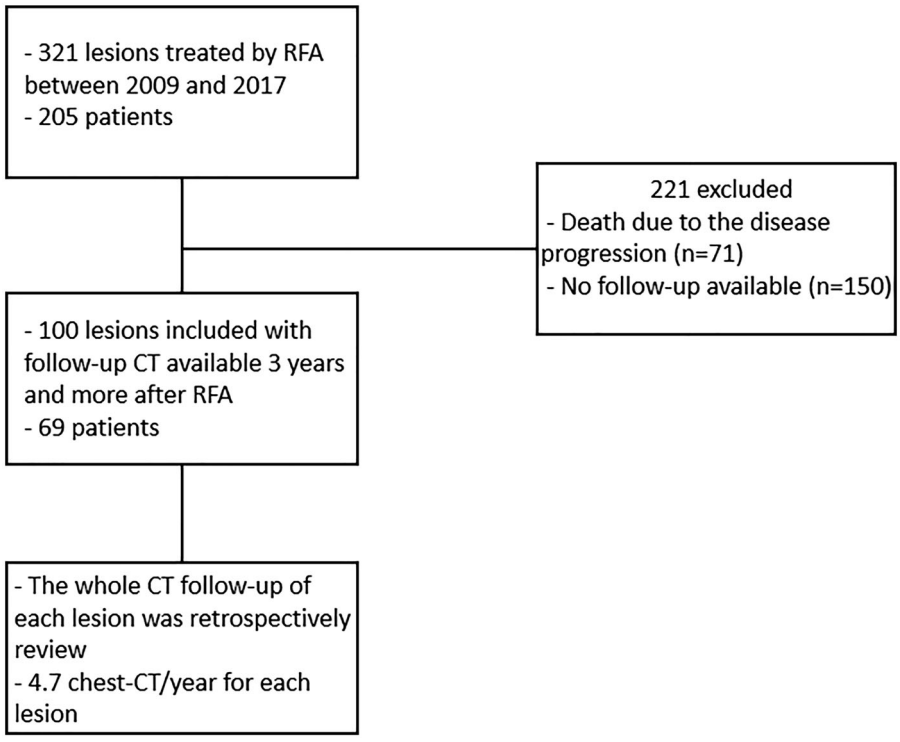

Figure 2. Flow chart of the study.

Table 1. Characteristics of patients and lesions..

	Numbers
Male	41 (41%)
Age (years)	62 ± 14 [23–88]
Lesion size (mm)	14 ± 7 [2–44]
Lesion size < 2 cm	83 (83%)
Pleural contact	18 (18%)
Distance from lesion to the chest wall (mm)	12 ± 12 [0–64]
RFA active portion needle size (mm)	29 ± 6 [20–40]
20	28 (28%)
30	49 (49%)
35	17 (17%)
40	6 (6%)
Power for first roll-off (W)	61 ± 40 [10–190]
Power for second roll-off (W)	56 ± 41 [5–200]
Average power for the 2 roll-offs (W)	59 ± 38 [8–195]
GGO surface area 48 h after RFA (mm^2)	884 ± 392 [271–1993]
Primary non-small cell lung cancer	16 (16%)
Metastatic disease	84 (84%)
Colorectal	29 (29%)
Sarcoma	37 (37%)
Thymus	5 (5%)
Esophagus	1 (1%)
Breast	2 (2%)
Thyroid	1 (1%)
Kidney	7 (7%)
Cylindroma	2 (2%)

This table represents the characteristics of patients and lesions.
GGO: ground-glass opacity; mm: millimeters; RFA: radiofrequency ablation.

Table 2. Proportion of different kind of scar over time.

Follow-up	Scars					Number of lesions
	Nodular	Fibrosis	Cavitary	Disappearance	Atelectasis	
1 year	56 (58%)	22 (23%)	9 (9%)	3 (3%)	6 (6%)	96
2 years	50 (54%)	26 (28%)	7 (8%)	4 (4%)	6 (6%)	93
3 years	46 (48%)	36 (38%)	5 (5%)	3 (3%)	6 (6%)	96
4 years	24 (34%)	33 (46%)	5 (7%)	4 (6%)	5 (7%)	71
5 years	16 (33%)	26 (53%)	4 (8%)	0 (0%)	3 (6%)	49
6 years	10 (30%)	20 (61%)	2 (6%)	0 (0%)	1 (3%)	33
7 years	6 (30%)	12 (60%)	2 (10%)	0 (0%)	0 (0%)	20

This table represents the evolution and proportions of different scar types over time.

radiofrequency needle than with the use of a 30-mm active radiofrequency needle ($p < 0.001$) (Figure 6).

Discussion

In most cases, morphological changes occurring during the long-term follow-up after lung RFA evolved into nodular scars in the first 3 years and into fibrosis after 3 years. Some nodular scars evolved with time to fibrosis. Atelectasis, fibrosis, and disappearance did not change with time. Power delivery was not a predictive factor for a specific pattern of the scar. Regarding predictive factors, a short distance to the pleura was predominantly associated with disappearance, and a needle diameter <30 mm was associated with atelectasis.

To date, indications, contraindications, advantages, and risks of lung RFA are well known; however, post-procedural monitoring has not yet been standardized. Recently, European guidelines for follow-up have been published not only for RFA but also for all types of ablation in interventional oncology [17]. Before these recommendations, Abtin et al. proposed a monitoring algorithm in 2012 [18] for patients undergoing positron emission tomography (PET)/CT, that included chest CT before treatment, CT at 1, 3, 6, 9, and 12 months after treatment, and then every 6 months in combination with PET at 3 and 9 months. PET/CT is proven to report false positives in mediastinal lymph nodes and needle insertion sites in the first 3 postoperative months. However, PET/CT may be a useful tool in incomplete treatment. The

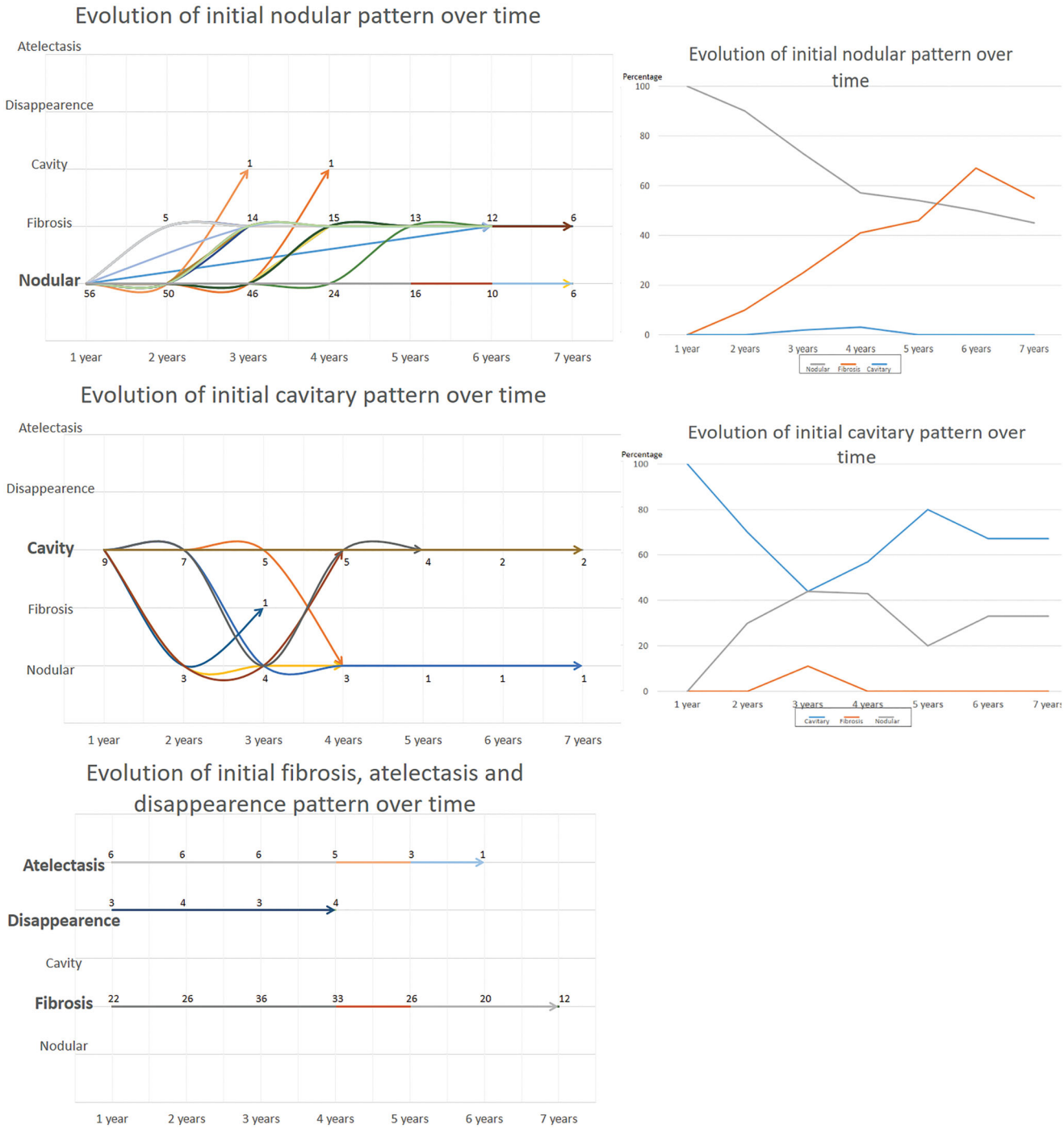

Figure 3. On the left side, the evolution of each kind of scar over time is represented. The top graph represents the evolution of the initial nodular pattern, The mid graph the evolution of initial cavitary pattern. On the lower graph has been merged the evolution of initial atelectasis, disappearance and fibrosis patterns. The figures correspond to the remaining lesions according to the follow-up duration. On the right side, curves show the proportion of the initial cavitary and nodular patterns over time.

authors reported that PET/CT after RFA is more useful for a global follow-up of the initial disease than for local recurrence [19,20]. The classification of different types of scars is key for a better follow-up of patients, allowing the early detection of an unusual local evolution or evolution with a risk of infection, such as cavitary scars [21].

Cavitary scars are associated with the risk of complications. Scars in the iatrogenic cavity predispose patients to hemoptysis or Aspergillus grafts, whose primary treatment is surgery [8]. When a cavity forms early after RFA, it is usually filled within a year. There was a trend toward cavitary scars when the treated lesions were close to the pleura. This finding can be explained by the fact that the closer the ablation zone is to the pleura, the smaller are the vessels. Since RFA causes occlusion of vessels <4 mm in diameter, necrosis can occur frequently [22].

Different factors, including early local changes after RFA, were studied to understand why some scars evolve in one way or another. Neither the locally delivered power nor the GGO area was a predictive factor for morphological

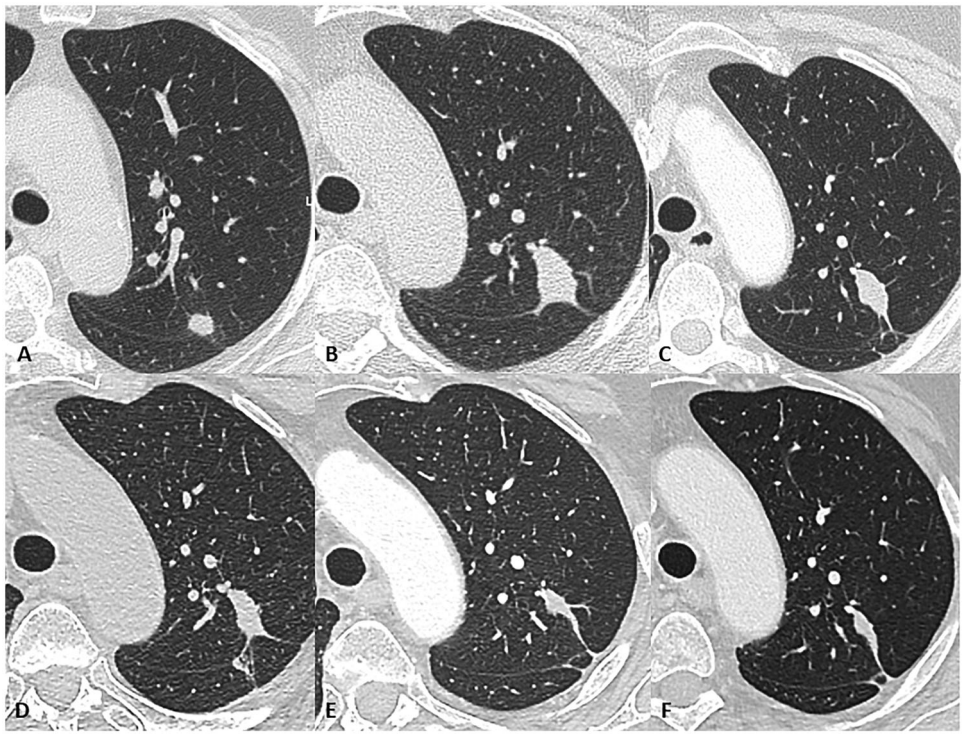

Figure 4. Example of the normal evolution of a scar with the nodular pattern that evolved into the fibrosis pattern over time. A. shows the lesion prior to treatment, and from B. to F. represents the lesion evolution each year for 5 years.

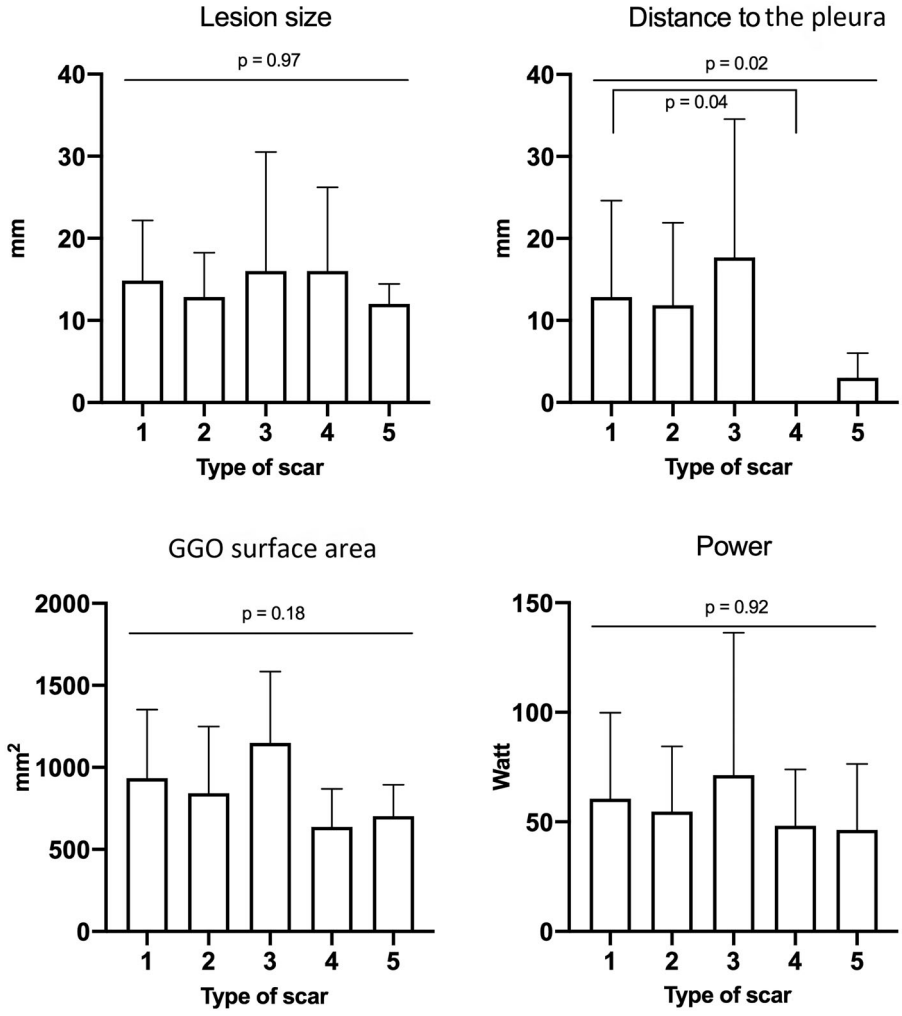

Figure 5. These diagrams show different parameters explored as etiologic factors for scar evolution. The only difference was observed between groups 1 and 4 and concerned the distance to the pleura. 1: nodular; 2: fibrosis; 3: cavitary; 4: disappearance; 5: atelectasis.

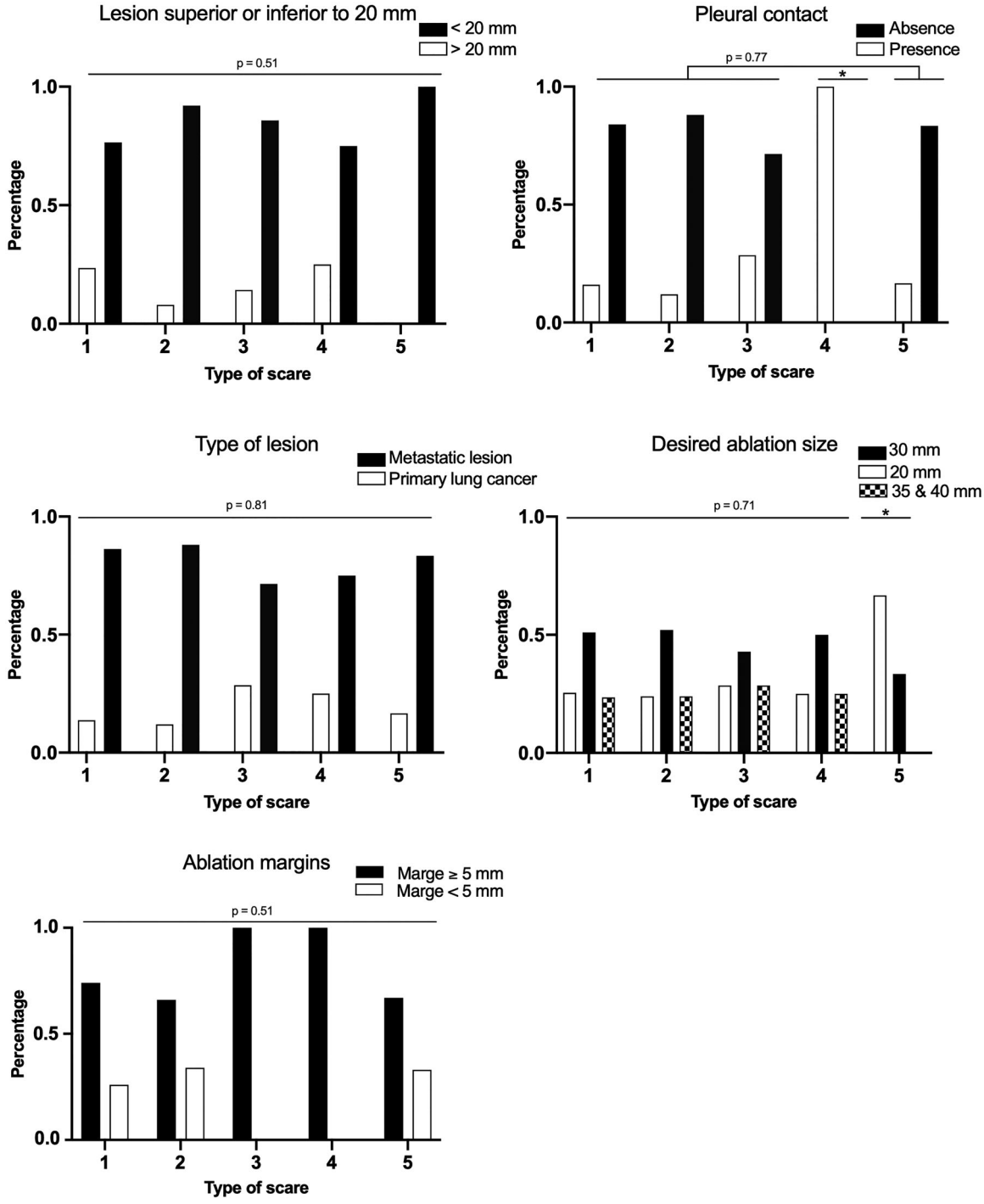

Figure 6. These diagrams show different parameters explored as etiologic factors for scar evolution. These qualitative parameters are presented as distributions in each group with percentages on order axis. 1: nodular; 2: fibrosis; 3: cavitary; 4: disappearance; 5: atelectasis. $^{*}p < 0.05$ compared with other groups.

evolution. A correlation exists between the destruction zone and delivered power. A study in pigs showed that the GGO observed on CT is the real ablation zone, and strong correlations (in millimeters) exist between the post-ablation diameters measured on *in vivo* chest CT and histological *ex vivo* measurements after explantation [23]. This GGO area corresponds to the ablation margin and should be 5 mm larger than the lesion on preoperative CT, which is easier to obtain with RFA than microwave ablation because of the round shape of RFA, in contrast to the oval shape of microwave ablation [24]. However, GGO assessment performed between 10 days and 2 months after RFA overestimates the long-term area of necrosis, as the ablated zone shrinks [23]. When shrinkage is complete, it results in scarring. Histological analysis of pigs' lungs after RFA showed a central zone of devascularization with necrosis and coagulation and a hematic peripheral crown in the short term (<1 week) and medium-term (approximately 2 months). The crown was enhanced after gadolinium injection due to inflammatory affluence. In the medium term, the edema subsided, and fibrosis was

observed in the central zone [25]. As these phenomena are always identical, some authors hypothesize that the type of scar depends highly on the local environment and that only lesions close to the pleura disappear.

Nodular scars represent an increase in the volume of the treated nodules in the initial months but are not indicators of local recurrence; some nodules regress, whereas others remain stable [14,26]. RFA is a physical attack on the lung, skirting the tumor, which leads to immunological phenomena. Schneider et al. studied the local and general immunological and inflammatory effects of RFA on human lungs; four patients were treated with RFA 10 days after surgery, with repeated blood samples collected before surgery, before RFA, and every 10 days for 3 months. Histologically, the authors found the accumulation of T cells and local inflammatory phenomena that could explain how some scars initially increased in size after treatment and then regressed. They hypothesized that these phenomena could serve as immunizations against long-term tumor recurrence [27].

We did not highlight one pattern that could predict local tumor progression. But in patients with 3 years of follow-up and more, corresponding to the selected population, we observed that the scar could be modified without local recurrence, especially in the first 3 years after RFA. In parallel, local recurrence and treatment failure are rarely more than 3 years after treatment that did not allow us to perform statistical analysis due to the few events. But interesting results in our point of view is the fibrosis, atelectasis, or disappearance patterns do not change with time, which mean if a fibrosis pattern evolves into a nodular, the probability of local recurrence is very high.

The main limitation of our study was that there was no systematic biopsy proving cancer in any of the treated lesions; however, all indications for RFA were established by a multidisciplinary team involving radiologists, thoracic surgeons, oncologists, pneumologists, radiation therapists, and pathologists. Another limitation was the heterogeneity of the different groups of scars; some types of scars were infrequent, and it was not easy to conduct long-term follow-up in these patients because most had a primary or metastatic disease with a poor outcome, which limited the follow-up.

This study described the long-term morphological evolution after lung RFA. It showed predominant evolution into nodular scars during the first 3 years, followed by predominant evolution into fibrosis. Fibrosis, disappearance, and atelectasis do not change with time, whereas nodular scars can evolve into fibrosis. Cavitary scars can fill and evolve into nodular scars. The distance close to the pleura was linked to the disappearance. Practitioners should describe scar evolution after RFA using this classification in follow-up reports to better monitor the evolution after lung RFA, for early detection of local recurrence, to homogenize practices, and to improve the reproducibility of studies.

Acknowledgments

Thanks to the LIIE team for their contribution.

Disclosure statement

No potential conflict of interest was reported by the author(s).

ORCID

Paul Habert http://orcid.org/0000-0003-2510-2727

References

[1] Simon CJ, Dupuy DE, DiPetrillo TA, et al. Pulmonary radiofrequency ablation: long-term safety and efficacy in 153 patients. Radiology. 2007;243(1):268–275.

[2] Yamazaki N, Watanabe H, XiaoWei L, et al. The relation between temperature distribution for lung RFA and electromagnetic wave frequency dependence of electrical conductivity with changing a lung's internal air volumes. Paper presented at the 2013 35th Annual International Conference of the IEEE Engineering in Medicine and Biology Society (EMBC); 2013 July 3–7; Osaka, Japan.

[3] Matsui Y, Hiraki T, Gobara H, et al. Radiation exposure of interventional radiologists during computed tomography fluoroscopy-guided renal cryoablation and lung radiofrequency ablation: direct measurement in a clinical setting. Cardiovasc Intervent Radiol. 2016;39(6):894–901.

[4] Greffier J, Ferretti G, Rousseau J, et al. National dose reference levels in computed tomography–guided interventional procedures—a proposal. Eur Radiol. 2020;30(10):5690–5701.

[5] Dupuy DE, Zagoria RJ, Akerley W, et al. Percutaneous radiofrequency ablation of malignancies in the lung. Am J Roentgenol. 2000;174(1):57–59.

[6] Kashima M, Yamakado K, Takaki H, et al. Complications after 1000 lung radiofrequency ablation sessions in 420 patients: a single center's experiences. Am J Roentgenol. 2011;197(4):W576–W580.

[7] Alexander ES, Hankins CA, Machan JT, et al. Rib fractures after percutaneous radiofrequency and microwave ablation of lung tumors: incidence and relevance. Radiology. 2013;266(3):971–978.

[8] Alberti N, Buy X, Frulio N, et al. Rare complications after lung percutaneous radiofrequency ablation: incidence, risk factors, prevention and management. Eur J Radiol. 2016;85(6):1181–1191.

[9] de Baère T, Aupérin A, Deschamps F, et al. Radiofrequency ablation is a valid treatment option for lung metastases: experience in 566 patients with 1037 metastases. Ann Oncol. 2015;26(5):987–991.

[10] Hasegawa T, Takaki H, Kodama H, et al. Three-year survival rate after radiofrequency ablation for surgically resectable colorectal lung metastases: a prospective multicenter study. Radiology. 2020;294(3):686–695.

[11] Benson AB, Venook AP, Al-Hawary MM, et al. Colon Cancer, Version 2.2021, NCCN clinical practice guidelines in oncology. J Natl Compr Canc Netw. 2021;19(3):329–359.

[12] Palussière J, Chomy F, Savina M, et al. Radiofrequency ablation of stage IA non–small cell lung cancer in patients ineligible for surgery: results of a prospective multicenter phase II trial. J Cardiothorac Surg. 2018;13(1):91.

[13] Modesto A, Giron J, Massabeau C, et al. Radiofrequency ablation for non-small-cell lung cancer in a single-lung patient: case report and review of the literature. Lung Cancer. 2013;80(3):341–343.

[14] Palussière J, Marcet B, Descat E, et al. Lung tumors treated with percutaneous radiofrequency ablation: computed tomography imaging follow-up. Cardiovasc Intervent Radiol. 2011;34(5):989–997.

[15] Ihara H, Gobara H, Hiraki T, et al. Radiofrequency ablation of lung tumors using a multitined expandable electrode: impact of the electrode array diameter on local tumor progression. J Vasc Interv Radiol. 2016;27(1):87–95.

[16] Anderson EM, Lees WR, Gillams AR. Early indicators of treatment success after percutaneous radiofrequency of pulmonary tumors. Cardiovasc Intervent Radiol. 2009;32(3):478–483.
[17] Maas M, Beets-Tan R, Gaubert J-Y, et al. Follow-up after radiological intervention in oncology: ECIO-ESOI evidence and consensus-based recommendations for clinical practice. Insights Imaging. 2020;11(1):83.
[18] Abtin FG, Eradat J, Gutierrez AJ, et al. Radiofrequency ablation of lung tumors: imaging features of the postablation zone. RadioGraphics. 2012;32(4):947–969.
[19] Deandreis D, Leboulleux S, Dromain C, et al. Role of FDG PET/CT and chest CT in the follow-up of lung lesions treated with radiofrequency ablation. Radiology. 2011;258(1):270–276.
[20] Schaefer O, Lohrmann C, Langer M. Diagnostic follow-up imaging: "Achilles heel" of performing radiofrequency heat ablation in lung malignancies. Eur J Radiol Extra. 2003;47(3):117–120.
[21] Okuma T, Matsuoka T, Yamamoto A, et al. Factors contributing to cavitation after CT-guided percutaneous radiofrequency ablation for lung tumors. J Vasc Interv Radiol. 2007;18(3):399–404.
[22] Steinke K, Haghighi KS, Wulf S, et al. Effect of vessel diameter on the creation of ovine lung radiofrequency lesions in vivo: preliminary results. J Surg Res. 2005;124(1):85–91.
[23] Yamamoto A, Nakamura K, Matsuoka T, et al. Radiofrequency ablation in a porcine lung model: correlation between CT and histopathologic findings. Am J Roentgenol. 2005;185(5):1299–1306.
[24] Kurilova I, Gonzalez-Aguirre A, Beets-Tan RG, et al. Microwave ablation in the management of colorectal cancer pulmonary metastases. Cardiovasc Intervent Radiol. 2018;41(10):1530–1544.
[25] Oyama Y, Nakamura K, Matsuoka T, et al. Radiofrequency ablated lesion in the normal porcine lung: long-term follow-up with MRI and pathology. Cardiovasc Intervent Radiol. 2005;28(3):346–353.
[26] Bojarski JD, Dupuy DE, Mayo-Smith WW. CT imaging findings of pulmonary neoplasms after treatment with radiofrequency ablation: results in 32 tumors. Am J Roentgenol. 2005;185(2):466–471.
[27] Schneider T, Hoffmann H, Dienemann H, et al. Immune response after radiofrequency ablation and surgical resection in nonsmall cell lung cancer. Semin Thorac Cardiovasc Surg. 2016;28(2):585–592.